

Description of double β decay within the continuum quasiparticle random-phase approximation

Vadim Rodin* and Amand Faessler†

Institute for Theoretical Physics, University of Tübingen, Auf der Morgenstelle 14, D-72076 Tübingen, Germany

(Received 19 July 2007; published 29 February 2008)

A method to calculate the nuclear double beta decay ($2\nu\beta\beta$ and $0\nu\beta\beta$) amplitudes within the continuum quasiparticle random phase approximation (cQRPA) is formulated. Calculations of the $\beta\beta$ transition amplitudes within the cQRPA are performed for ^{76}Ge , ^{100}Mo , and ^{130}Te . A rather simple nuclear Hamiltonian consisting of a phenomenological mean field and a zero-range residual particle-hole and particle-particle interaction is used. The calculated $2\nu\beta\beta$ amplitudes are almost unaffected when the single-particle continuum is taken into account, whereas we find a regular suppression of the $0\nu\beta\beta$ amplitudes that can be associated with additional ground-state correlations owing to collective states in the continuum. It is expected that inclusion of nucleon pairing in the single-particle continuum will somewhat compensate this suppression.

DOI: [10.1103/PhysRevC.77.025502](https://doi.org/10.1103/PhysRevC.77.025502)

PACS number(s): 23.40.-s, 21.60.Jz, 27.50.+e, 27.60.+j

I. INTRODUCTION

Neutrino oscillation experiments have proven that neutrinos are massive particles (see, e.g., Ref. [1]). However, the absolute scale of the neutrino masses cannot in principle be deduced from the observed oscillations. To determine the absolute neutrino masses down to the level of tens of meV, study of the neutrinoless double beta decay ($0\nu\beta\beta$) becomes indispensable. Furthermore, this process, which violates the total lepton number by two units, is an *experimentum crucis* to reveal the Majorana nature of neutrinos [2–5].

The next generation of experiments (GERDA, CUORE, SuperNEMO, etc.) has a great discovery potential for observation of $0\nu\beta\beta$ decay and for providing reliable measurements of the corresponding lifetimes. The determination of the effective Majorana mass (or relevant GUT and SUSY parameters depending on what mechanism of the $0\nu\beta\beta$ decay dominates) from experimental data can be only as good as the knowledge of the nuclear matrix elements $M^{0\nu}$ on which the $0\nu\beta\beta$ decay rates depend. Thus, a better understanding of the nuclear structure effects important for describing the matrix elements is needed to interpret the data accurately. It is crucial in this connection to develop theoretical methods capable of reliably evaluating the nuclear matrix elements, and to realistically assess their uncertainties.

At present, the most elaborate analysis of the uncertainties in the $0\nu\beta\beta$ decay nuclear matrix elements $M^{0\nu}$ calculated within the quasiparticle random phase approximation (QRPA) and the renormalized quasiparticle random phase approximation (RQRPA) has been performed in recent papers [6,7]. The experimental $2\nu\beta\beta$ decay rates have been used there to adjust the most relevant parameter, the strength g_{pp} of the particle-particle interaction. The major observation of Refs. [6,7] is that such a procedure makes the calculated $M^{0\nu}$ essentially independent of the size of the single-particle (s.p.) basis of the QRPA (the bases comprising $N = 2, 3$, and 5 major oscillator shells were used). Furthermore, the matrix elements

have been demonstrated to also become rather stable with respect to the possible quenching of the axial vector coupling constant g_A .

The calculations in Refs. [6,7] were performed within “the standard QRPA” scheme in which a discrete s.p. basis and the harmonic oscillator wave functions as the s.p. wave functions are used to build the BCS ground state and the spectrum of the excited states. Keeping in mind that many multipoles contribute appreciably to $M^{0\nu}$, one can *a priori* expect that enlargement of the model space should lead to more accurate matrix elements $M^{0\nu}$. (In other words, any basis truncation leads to an uncertainty.) This should be contrasted with the case of the $2\nu\beta\beta$ amplitude to which only Gamow-Teller transitions contribute and a s.p. basis of $N = 1$ –2 major shells is good enough. In this respect, it would be interesting to test the stability of the calculated $M^{0\nu}$ found in Refs. [6,7] by letting $N \rightarrow \infty$. Thus, if one could include the entire s.p. basis into the calculation scheme, the question about the dependence of the QRPA results on size of the s.p. basis as a source of the uncertainties in the calculated $M^{0\nu}$ would become irrelevant.

There is no problem within the QRPA for including low-lying major shells composed of bound s.p. states into the model space. But inclusion of major shells lying much higher than the Fermi level immediately encounters principal limitations of approximation of the continuum of unbound s.p. states by discrete levels. Basically, only one major shell, lying higher than the Fermi shell (already containing quasistationary states), can safely be considered.

The only possible way to treat properly the s.p. continuum is provided within the continuum quasiparticle random phase approximation (cQRPA). The continuum random phase approximation (cRPA) was formulated about 30 years ago in the pioneering work of Shlomo and Bertsch [8] and since then has been used to successfully describe structure and decay properties of various giant resonances [9], muon capture [10], and neutrino-nucleus reactions with large momentum transfer [11]. To apply the cRPA in open-shell nuclei one has to take nucleon pairing into consideration. This requires development of a quasiparticle version of the cRPA, namely, a continuum QRPA approach. Such a cQRPA approach to

*vadim.rodin@uni-tuebingen.de

†amand.faessler@uni-tuebingen.de

describing charge-exchange excitations has been developed in Refs. [12,13].

The cQRPA provides a regular way of using realistic wave functions of unbound s.p. states in terms of the s.p. Green's functions without the need to approximate them by the oscillator ones. Moreover, having an alternative formulation of the QRPA can help to understand current QRPA results and their deficiencies.

Two principal effects of taking into account the s.p. continuum within the proton-neutron QRPA (pn-QRPA), which affect the calculated values of $M^{0\nu}$ in an opposite way, can be expected. First, additional ground-state (g.s.) correlations can appear because of collective multipole states in the continuum, which generally have a tendency to decrease $M^{0\nu}$. Second, pairing in the continuum can increase $0\nu\beta\beta$ matrix element $M^{0\nu}$ (see the relevant discussion in Ref. [14]).

The principal aim of this work is to formulate for the first time a nuclear structure framework for calculating the double beta decay matrix elements $M^{2\nu}$ and $M^{0\nu}$ within the cQRPA and to test within this method the stability of the calculated $M^{0\nu}$ found in Refs. [6,7]. As a first step, a simpler version of the cQRPA with nucleon pairing realized only on a discrete basis is applied in the present work; therefore, the calculated $M^{0\nu}$ values of this paper should be considered lower limits for the matrix elements within the cQRPA. To consistently include nucleon pairing in the continuum within the cQRPA is a formidable task and is postponed to future publications.

We merely focus here on a qualitative discussion of the relative effect obtained within the cQRPA in comparison with the standard discrete QRPA. Therefore, the $M^{0\nu}$ values of the present work may be somewhat different from those of Refs. [6,7] since we have not implemented the most elaborate representation for the neutrino potential (modified by the finite nucleon size correction, higher order terms of the nucleon weak current, etc.; see, e.g., Ref. [7]). The nucleon-nucleon short-range correlations (SRC) are implemented here in the usual way, in terms of the Jastrow-like functions [15]. This, however, might lead to an overestimation of the effect of the SRC (see the recent discussion in Refs. [14,16]).

The paper is organized as follows: The pn-QRPA equations in the coordinate presentation and the way to take into account the s.p. continuum in them are given in the first two parts of Sec. II. In the latter two parts of that section formulas for calculating strength functions and $M^{2\nu}$ and $M^{0\nu}$ are presented. In Sec. III we present the results and we give conclusions in Sec. IV.

II. CONTINUUM QRPA

Since its formulation in the pioneering work of Shlomo and Bertsch [8], the cRPA has long been used to successfully describe structure and decay properties of various giant resonances and their high-lying overtones embedded in the single-particle continuum. The structure of the overtones is formed by the s.p. excitations changing the s.p. radial quantum number (which correspond to transitions over two or more major shells). Their contribution to the nuclear

multipole response is marked if probe operators have nontrivial radial dependence, which is the case, for example, for muon capture [10] and neutrino-nucleus reactions with large momentum transfer [11]. The direct nucleon decay of various giant resonances and their overtones has been extensively analyzed within the cRPA by Urin and collaborators (see, e.g., Ref. [9]).

To apply the cRPA in open-shell nuclei one has to take nucleon pairing into consideration. This requires development of a quasiparticle version of the cRPA, namely, the cQRPA approach. The approach should account for the important influence of the residual particle-particle (p-p) interaction along with the particle-hole (p-h) one included within the usual cRPA. Such a cQRPA approach based on the coordinate space Hartree-Fock-Bogolyubov formalism has been formulated and applied recently to describe strength functions of different multipole excitations without charge exchange [17].

A pn-cQRPA approach to describing charge-exchange excitations was developed in Ref. [12] and, independently, in Ref. [13]. In Ref. [18] the approach was applied to analyze the low-energy part of the Gamow-Teller (GT) strength distribution relevant for description of single beta decay in astrophysical applications. In Ref. [13] the Fermi and GT strength distributions in semimagic nuclei were described within a wide excitation-energy interval that includes the overtones of the IAS and GTR, the so-called monopole and spin-monopole resonances.

In describing the $0\nu\beta\beta$ decay, some transition strength into the s.p. continuum is missing within the standard QRPA calculation scheme, especially for the high-multipole excitations with $L \geq 2$ (compare, e.g., with the description of muon capture where the contribution of the highly excited giant resonances dominates [10]). The contribution of these multipoles to $M^{0\nu}$ becomes particularly important because the monopole (Fermi and Gamow-Teller) contributions are suppressed by symmetry constraints. (See, e.g., the multipole decomposition of $M^{0\nu}$ in Fig. 5 of Ref. [7]; for a recent general discussion of how the SU(4)-symmetry violation by the residual p-p interaction affects $M^{2\nu}$ see Ref. [19].) Thus, $M^{0\nu}$ gets strongly suppressed by the g.s. correlations, short-range correlations, etc.; therefore fine effects (such as influence of the s.p. continuum) can be expected to come into play. The first attempt to briefly describe the $\beta\beta$ observables within the pn-cQRPA was undertaken in Ref. [20].

A. pn-QRPA equations in coordinate representation

The system of homogeneous equations for the forward and backward amplitudes $X_{\pi\nu}^{(J^\pi s)}$ and $Y_{\pi\nu}^{(J^\pi s)}$, respectively, is usually solved to calculate the energies ω_s and the wave functions $|J^\pi M, s\rangle$ of excited states in isobaric odd-odd nuclei within the pn-QRPA (see, e.g., Refs. [2,21]; here "s" labels the different QRPA states). However, it is impossible to handle an infinite number of amplitudes X, Y if one wants to include the continuum of unbound s.p. states. Instead, by going into the

coordinate representation the pn-QRPA can be reformulated in equivalent terms of four-component radial transition density $\{\varrho_{I,s}^{(JLS)}\}$ ($I = 1, \dots, 4$) defined for each state $|J^\pi M, s\rangle$. The components are determined by the standard QRPA amplitudes X and Y as follows:

$$\varrho_{I,s}^{(JLS)}(r) = \sum_{\pi v} R_{I,s}^{\pi v} \chi_{\pi v}(r), \quad (1)$$

$$\begin{pmatrix} R_{p-h}^{\pi v} \\ R_{h-p}^{\pi v} \\ R_{p-p}^{\pi v} \\ R_{h-h}^{\pi v} \end{pmatrix}_s = \begin{pmatrix} u_\pi v_\nu X_{\pi\nu} + v_\pi u_\nu Y_{\pi\nu} \\ u_\pi v_\nu Y_{\pi\nu} + v_\pi u_\nu X_{\pi\nu} \\ u_\pi u_\nu X_{\pi\nu} - v_\pi v_\nu Y_{\pi\nu} \\ u_\pi u_\nu Y_{\pi\nu} - v_\pi v_\nu X_{\pi\nu} \end{pmatrix}_s,$$

where u and v are the coefficients of Bogolyubov transformation and $\chi_{\pi v}(r) = t_{(\pi)(v)}^{(JLS)} \chi_\pi(r) \chi_\nu(r)$ with $(\pi) = (j_\pi l_\pi)[(v) = (j_\nu l_\nu)]$ and $r^{-1} \chi_\pi(r) [r^{-1} \chi_\nu(r)]$ being the s.p. proton (neutron) quantum numbers and radial wave functions, respectively. In Eq. (1) the spin-angular variables are already separated out since the nuclear response to a probe operator having definite spin-angular symmetry determined by the irreducible spin-angular tensor $T_{JLSM}(\mathbf{n})$ is calculated, and $t_{(\pi)(v)}^{(JLS)} = \frac{1}{\sqrt{2J+1}} \langle \pi \| T_{JLS} \| \nu \rangle$ represents the corresponding reduced matrix element. Hereafter, we shall systematically omit the superscript “(JLS)” when it does not lead to confusion.

According to the definition of Eq. (1), the elements ϱ_1 , ϱ_2 , ϱ_3 , and ϱ_4 can be called the particle-hole, hole-particle, particle-particle, and hole-hole components of the transition density, respectively, and can be generally considered as a four-dimensional vector: $\{\varrho_I^J\}$. In particular, the transition matrix element to a state $|s, JM\rangle$ corresponding to a particle-hole operator

$$\hat{V}_{JLSM}^{(-)} = \sum_a \mathbf{V}_{JLSM}(\mathbf{x}_a) \tau_a^-, \quad (2)$$

$$\mathbf{V}_{JLSM}(\mathbf{x}_a) = V_{(JLS)}(r_a) T_{JLSM}(\mathbf{n}_a) \quad (3)$$

is determined by a one-dimensional integral of the product of the element ϱ_1 and the radial dependence of the operator [Eqs. (2) and (3)]:

$$\langle J^\pi M | \hat{V}_{JLSM}^{(-)} | 0 \rangle = \int \varrho_1^{(JLS)}(r) V_{(JLS)}(r) dr. \quad (4)$$

The pn-QRPA system of integral equations for the elements $\varrho_{I,s}^{(JLS)}$ follows from the standard pn-QRPA equations for the X and Y amplitudes (see, e.g., Refs. [2,21]) by making use of the definition from Eq. (1):

$$\varrho_{I,s}^{(JLS)}(r) = \sum_K \int A_{IK}^{(JLS)}(rr', \omega = \omega_s) \times F_K^{(JLS)}(r'r'') \varrho_{K,s}^{(JLS)}(r'') dr' dr''. \quad (5)$$

Here, $(rr')^{-1} F_K^{(JLS)}(r, r')$ is the radial part of the residual interaction in the K channel (where $K = 1, 2$ for the p-h channel and $K = 3, 4$ for the p-p channel and the so-called symmetric approximation is used here). The 4×4 matrix $(rr')^{-1} A_{IK}(r_1 r_2, \omega)$ is the radial part of the free

two-quasiparticle propagator (response function):

$$A_{IK}(r_1 r_2, \omega) = \sum_{\pi v} A_{IK}^{\pi v}(\omega) \chi_{\pi v}(r_1) \chi_{\pi v}(r_2),$$

$$A_{KI}^{\pi v} = A_{IK}^{\pi v},$$

$$A_{11}^{\pi v} = \frac{u_\pi^2 v_\nu^2}{\omega - E_{\pi\nu}} + \frac{u_\nu^2 v_\pi^2}{-\omega - E_{\pi\nu}},$$

$$A_{33}^{\pi v} = \frac{u_\pi^2 u_\nu^2}{\omega - E_{\pi\nu}} + \frac{v_\nu^2 v_\pi^2}{-\omega - E_{\pi\nu}},$$

$$A_{13}^{\pi v} = u_\nu v_\nu \left(\frac{u_\pi^2}{\omega - E_{\pi\nu}} - \frac{v_\pi^2}{-\omega - E_{\pi\nu}} \right), \quad (6)$$

$$A_{14}^{\pi v} = -u_\pi v_\pi \left(\frac{v_\nu^2}{\omega - E_{\pi\nu}} - \frac{u_\nu^2}{-\omega - E_{\pi\nu}} \right),$$

$$A_{12}^{\pi v} = -A_{34}^{\pi v} = \frac{u_\pi v_\pi v_\nu u_\nu}{\omega - E_{\pi\nu}} + \frac{u_\pi v_\pi v_\nu u_\nu}{-\omega - E_{\pi\nu}},$$

$$A_{22}^{\pi v}(\omega) = A_{11}^{\pi v}(-\omega), \quad A_{44}^{\pi v}(\omega) = A_{33}^{\pi v}(-\omega),$$

$$A_{23}^{\pi v}(\omega) = A_{14}^{\pi v}(-\omega), \quad A_{24}^{\pi v}(\omega) = A_{13}^{\pi v}(-\omega),$$

with $E_{\pi\nu} = E_\pi + E_\nu$, where E_π and E_ν are the proton and neutron quasiparticle energy, respectively. The expressions for the elements of the free two-quasiparticle propagator A_{IK} can also be obtained by making use of the regular and anomalous s.p. Green's functions for Fermi systems with nucleon pairing (see, e.g., Ref. [13]), in an analogous way to that described in the monograph [22] for response of Fermi systems to a s.p. probe operator acting in the neutral channel.

These equations allow a compact schematic representation when the spin-angular variables are not separated out. In such a case, the substitutions $r_a \rightarrow \mathbf{x}_a$, $\chi_\alpha(r) \rightarrow \chi_\alpha(\mathbf{x})$, $\varrho \rightarrow \boldsymbol{\varrho}$, $A_{IK} \rightarrow \mathbf{A}_{IK}$, and $F_K \rightarrow \mathbf{F}_K$ have to be made and the factor $t^{(JLS)}$ should be omitted in the formulas. Then, schematically denoting the double integration over \mathbf{x}' , \mathbf{x}'' in Eq. (5) as $\{\dots\}$, one can rewrite the equation as

$$\boldsymbol{\varrho}_I = \{\mathbf{A}_{IK} \mathbf{F}_K \boldsymbol{\varrho}_K\}, \quad (7)$$

where summation over the repeated index K on the right-hand side is assumed.

The total two-quasiparticle propagator (two-quasiparticle Green function) \tilde{A} that includes the QRPA iterations of the p-h and p-p interactions is very useful in practical applications. It satisfies an integral equation of the Bethe-Salpeter type $\tilde{A}_{IK} = \mathbf{A}_{IK} + \{\mathbf{A}_{IK} \mathbf{F}_K \tilde{A}_{K'K}\}$:

$$\tilde{A}_{IK}^{(JLS)}(rr', \omega) = A_{IK}^{(JLS)}(rr', \omega) + \sum_{K'} \int A_{IK'}^{(JLS)}(rr_1, \omega) \times F_{K'}^{(JLS)}(r_1 r_2) \tilde{A}_{K'K}^{(JLS)}(r_2 r', \omega) dr_1 dr_2. \quad (8)$$

The following spectral decompositions hold for the radial components $\tilde{A}_{11}(\omega)$, $\tilde{A}_{12}(\omega)$, and $\tilde{A}_{22}(\omega)$:

$$\tilde{A}_{11}(r_1 r_2, \omega) = \sum_s \frac{\varrho_1^s(r_1) \varrho_1^s(r_2)}{\omega - \omega_s + i\delta} - \sum_s \frac{\varrho_2^s(r_1) \varrho_2^s(r_2)}{\omega + \omega_s - i\delta},$$

$$\tilde{A}_{22}(r_1 r_2, \omega) = \tilde{A}_{11}(r_1 r_2, -\omega), \quad (9)$$

$$\tilde{A}_{12}(r_1 r_2, \omega) = \sum_s \frac{\varrho_1^s(r_1) \varrho_2^s(r_2)}{\omega - \omega_s + i\delta} - \sum_s \frac{\varrho_2^s(r_1) \varrho_1^s(r_2)}{\omega + \omega_s - i\delta}.$$

These components are the only ones that will be needed in the following for description of single and double beta decay transition probabilities. The spectral decompositions for the other elements of \tilde{A} can readily be written down in analogy to Eqs. (9). Thus, one sees from Eqs. (9) that all the information about the QRPA solutions [energies ω_s and transition densities $\varrho_{l,s}(r)$] resides in the poles of the total two-quasiparticle propagator \tilde{A} .

In this paper, the residual isovector particle-hole interaction and the particle-particle interaction in both the neutral (pairing) and charge-exchange channels are chosen in the form of the Landau-Migdal forces of zero range (proportional to the spatial δ function) [22], which is similar to the choice of Refs. [23,24]. The effective isovector particle-hole interaction \mathbf{F}_K (for $K = 1, 2$) is given by

$$\mathbf{F}_K(\mathbf{x}_1, \mathbf{x}_2) = C_0(f_{\text{ph}}^0 + f_{\text{ph}}^1 \boldsymbol{\sigma}_1 \cdot \boldsymbol{\sigma}_2) \boldsymbol{\tau}_1 \cdot \boldsymbol{\tau}_2 \delta(\mathbf{r}_1 - \mathbf{r}_2), \quad (10)$$

where f_{ph}^0 and f_{ph}^1 are the phenomenological Landau-Migdal parameters. Hereafter, all the strength parameters of the residual interactions are given in units of $C_0 = 300 \text{ MeV fm}^3$.

The residual p-p interaction \mathbf{F}_K (for $K = 3, 4$) is given by a similar expression:

$$\mathbf{F}_K(\mathbf{x}_1, \mathbf{x}_2) = -C_0(g_{\text{pp}}^0 + g_{\text{pp}}^1 \boldsymbol{\sigma}_1 \cdot \boldsymbol{\sigma}_2) \delta(\mathbf{r}_1 - \mathbf{r}_2), \quad (11)$$

and the pairing interaction is

$$\mathbf{F}^{\text{pair}}(\mathbf{x}_1, \mathbf{x}_2) = -C_0 g^{\text{pair}} \delta(\mathbf{r}_1 - \mathbf{r}_2). \quad (12)$$

The pairing strengths g_n^{pair} and g_p^{pair} for neutron and proton subsystems are fixed within the BCS model to reproduce the experimental neutron and proton pairing energies. All the other strength parameters in the particle-particle channel are always given relative to $(g_n^{\text{pair}} + g_p^{\text{pair}})/2$.

B. Taking the single-particle continuum into consideration

The coordinate-space version of the pn-QRPA described in the preceding section is especially suitable for taking the s.p. continuum into consideration. But before proceeding with the continuum, it is worth noting that if one lets the double sums in Eq. (6) run just over finite sets of proton and neutron s.p. states, the presented version of the pn-QRPA is fully equivalent to the usual “discrete” one, which is formulated in terms of X and Y amplitudes. We make use of this fact to check the calculation scheme by comparing “discrete” QRPA results calculated in these two different, but formally equivalent, ways. As anticipated, the results are the same within the accuracy of the numerical techniques used.

To take the s.p. continuum into consideration, the double-sum representation for the free response function [Eq. (6)] should be transformed according to the following prescription:

- (i) The Bogolyubov coefficients v_α, u_α and the quasiparticle energies E_α are approximated by their non-pairing values $v_\alpha = 0, u_\alpha = 1$, and $E_\alpha = \varepsilon_\alpha - \lambda_i$ for those s.p. states in the s.p. continuum that lie far up of the chemical potential λ_i [i.e., $\varepsilon_\alpha - \lambda_i \gg \Delta_\alpha$, where $i = p$ (protons) or n (neutrons)]. The accuracy of this approximation is $\frac{\Delta}{|\varepsilon - \lambda|}$, which is good enough already for $\varepsilon_\alpha - \lambda_i \geq E_{\text{max}} \simeq 10 \text{ MeV}$.

The usual BCS representations for v_α, u_α , and E_α are taken for all the other s.p. states with $\varepsilon_\alpha - \lambda_i < E_{\text{max}}$.

- (ii) The radial single-particle Green’s function

$$g_{(\omega)}(r_1 r_2, \varepsilon) = \sum_{\alpha_r} \frac{\chi_\alpha(r_1) \chi_\alpha(r_2)}{\varepsilon - \varepsilon_\alpha + i\delta}$$

is used to explicitly perform the sum over the s.p. states in the continuum. Here, the sum \sum_{α_r} runs over different radial quantum numbers for a given spin-angular symmetry (α). The Green’s function satisfies the inhomogeneous radial s.p. Schrödinger equation $[h_{0(\alpha)}(r) - \varepsilon]g_{(\omega)}(r r', \varepsilon) = -\delta(r - r')$ and can be constructed as a product of regular and irregular solutions of the homogeneous equation $[h_{0(\alpha)}(r) - \varepsilon]\chi_{(\alpha)}^{\text{reg, irreg}}(r, \varepsilon) = 0$ (see, e.g., Refs. [8,21]).

As a result, we get from Eq. (6) the following representation for the components A_{IK} of the free two-quasiparticle propagator:

$$\begin{aligned} A_{11}(r_1 r_2, \omega) &= \sum_{v_<, \pi_<} \frac{v_v^2 u_\pi^2}{\omega - E_{\pi v}} \chi_{\pi v}(r_1) \chi_{\pi v}(r_2) + \sum_{v_<, (\pi)} (t_{(\pi)(v)}^{JLS})^2 \\ &\quad \times v_v^2 \chi_v(r_1) \chi_v(r_2) g'_{(\pi)}(r_1 r_2, \lambda_p + \omega - E_v) \\ &\quad + \{\pi \leftrightarrow v, \omega \rightarrow -\omega\}, \\ A_{12}(r_1 r_2, \omega) &= \sum_{v_<, \pi_<} u_v v_v u_\pi v_\pi \left[\frac{1}{\omega - E_{\pi v}} + \frac{1}{-\omega - E_{\pi v}} \right] \\ &\quad \times \chi_{\pi v}(r_1) \chi_{\pi v}(r_2), \\ A_{13}(r_1 r_2, \omega) &= \sum_{v_<, \pi_<} u_v v_v \left[\frac{u_\pi^2}{\omega - E_{\pi v}} + \frac{v_\pi^2}{-\omega - E_{\pi v}} \right] \\ &\quad \times \chi_{\pi v}(r_1) \chi_{\pi v}(r_2) + \sum_{v_<, (\pi)} (t_{(\pi)(v)}^J)^2 u_v v_v \chi_v(r_1) \\ &\quad \times \chi_v(r_2) g'_{(\pi)}(r_1 r_2, \lambda_p + \omega - E_v), \\ A_{33}(r_1 r_2, \omega) &= \sum_{v_<, \pi_<} \left[\frac{u_\pi^2 u_\pi^2}{\omega - E_{\pi v}} + \frac{v_\pi^2 v_\pi^2}{-\omega - E_{\pi v}} \right] \chi_{\pi v}(r_1) \\ &\quad \times \chi_{\pi v}(r_2) + \sum_{v_<, (\pi)} (t_{(\pi)(v)}^J)^2 u_v^2 \chi_v(r_1) \chi_v(r_2) g'_{(\pi)} \\ &\quad \times (r_1 r_2, \lambda_p + \omega - E_v) + \sum_{\pi_<, (v)} (t_{(\pi)(v)}^J)^2 u_\pi^2 \\ &\quad \times \chi_\pi(r_1) \chi_\pi(r_2) g'_{(v)}(r_1 r_2, \lambda_n + \omega - E_\pi), \\ A_{44}(\omega) &= A_{33}(-\omega), \quad A_{14}(\omega) = A_{13}(-\omega, \pi \leftrightarrow v), \\ A_{24}(\omega) &= A_{13}(-\omega), \quad A_{23}(\omega) = A_{13}(\omega, \pi \leftrightarrow v), \end{aligned} \quad (13)$$

where $\pi_<(v_<)$ means $\pi \leq \pi_{\text{max}}(v \leq v_{\text{max}})$, $\pi_{\text{max}}(v_{\text{max}})$ is the s.p. state with the largest energy included in the BCS basis for which $E_{\pi_{\text{max}}} = \varepsilon_{\pi_{\text{max}}} - \lambda_p (E_{v_{\text{max}}} = \varepsilon_{v_{\text{max}}} - \lambda_n)$ with the acceptable accuracy as previously described, and

$$g'_{(\pi)}(r_1 r_2, \varepsilon) = g_{(\pi)}(r_1 r_2, \varepsilon) - \sum_{\pi_r <} \frac{\chi_\pi(r_1) \chi_\pi(r_2)}{\varepsilon - \varepsilon_\pi} \quad (14)$$

is the subtracted radial s.p. Green’s function (the Green’s function from which the contribution of all discrete s.p. states

and those quasidiscrete s.p. states included in the BCS basis is subtracted).

C. Strength functions

Different strength functions can be readily calculated in terms of the imaginary part of the total two-quasiparticle propagator $\text{Im}\tilde{A}$. The strength function corresponding to a charge-exchange single-particle operator $V_{J\mu}^{(\mp)}$ acting in the $\beta^{(\mp)}$ channel,

$$\hat{V}_{JLSM}^{(\mp)} = \sum_a \mathbf{V}_{JLSM}(\mathbf{x}_a) \tau_a^{(\mp)}, \quad (15)$$

where $\mathbf{V}_{JLSM}(\mathbf{x}_a)$ is given by Eq. (3), is defined by the usual expression:

$$S^{(\mp)}(\omega) = \sum_s |(J^\pi M, s | \hat{V}_{JLSM}^{(\mp)} | 0\rangle|^2 \delta(\omega - \omega_s^\mp),$$

with $\omega_s^\mp = E_s^\mp - E_0$ being the excitation energy of the corresponding isobaric nucleus ($N \mp 1, Z \pm 1$) relative to the ground state $|0\rangle$ of the parent nucleus (N, Z) with energy E_0 . Making use of the spectral decomposition [Eqs. (9)] one can easily verify the following integral representations of the strength functions:

$$S^{(-)}(\omega^-) = -\frac{1}{\pi} \{\mathbf{V}\tilde{A}_{11}(\omega)\mathbf{V}\} = -\frac{1}{\pi} \text{Im} \int V_{(JLS)} \times (r_1) \tilde{A}_{11}^{(JLS)}(r_1 r_2; \omega) V_{(JLS)}(r_2) dr_1 dr_2, \quad (16)$$

$$S^{(+)}(\omega^+) = -\frac{1}{\pi} \{\mathbf{V}\tilde{A}_{22}(\omega)\mathbf{V}\} = -\frac{1}{\pi} \text{Im} \int V_{(JLS)} \times (r_1) \tilde{A}_{22}^{(JLS)}(r_1 r_2; \omega) V_{(JLS)}(r_2) dr_1 dr_2, \quad (17)$$

where $\omega^\mp = \omega \pm (\lambda_p - \lambda_n) \pm (m_n - m_p)$ represents the calculated excitation energy relative to the g.s. of the parent nucleus and m_p and m_n are the proton and neutron masses. The pn-QRPA excitation spectrum, originally calculated in terms of ω , gets a constant energy shift to be represented in terms of ω^\mp , because the modified nuclear Hamiltonian $\hat{H} - \lambda_p \hat{Z} - \lambda_n \hat{N}$ (as in the BCS model) is used within the QRPA and the model nuclear Hamiltonian does not contain the rest energies of nucleons.

One can also define a nondiagonal strength function as

$$S_V^{(--)}(\omega) = \sum_s \langle 0' | \hat{V}_{JLS\bar{M}}^{(-)} | J^\pi M, s \rangle \langle J^\pi M, s | \hat{V}_{JLSM}^{(-)} | 0 \rangle \delta(\omega - \omega'_s), \quad (18)$$

with $\bar{\omega}_s = E_s - (E_0 + E_{0'})/2 = (\omega_s^- + \omega_s^+)/2$ and $\hat{V}_{JLS\bar{M}}^{(-)}$ being the time reverse of $\hat{V}_{JLSM}^{(-)}$. Such a strength function is closely related to the amplitude of the $2\nu\beta\beta$ decay, when $|0\rangle$ and $|0'\rangle$ are the g.s. wave functions of the initial (decaying) and final (product) nuclei, respectively.

To calculate $S_V^{(--)}(\omega)$ within the pn-QRPA one faces the usual problem that the spectrum $|s\rangle$ comes out slightly different when calculated with respect to $|0\rangle$ or $|0'\rangle$. Identifying the

QRPA vacuum $|0'\rangle$ with that of $|0\rangle$, one gets $\bar{\omega}_s = \omega_s$ and

$$S^{(--)}(\omega) = -\frac{1}{\pi} \{\mathbf{V}\tilde{A}_{12}(\omega)\mathbf{V}\} = -\frac{1}{\pi} \text{Im} \int V_{(JLS)}(r_1) \tilde{A}_{12}^{(JLS)} \times (r_1 r_2; \omega) V_{(JLS)}(r_2) dr_1 dr_2 \quad (19)$$

or, alternatively, identifying $|0\rangle$ with $|0'\rangle$

$$S^{(--)}(\omega) = -\frac{1}{\pi} \{\mathbf{V}\tilde{A}'_{12}(\omega)\mathbf{V}\} = -\frac{1}{\pi} \text{Im} \int V_{(JLS)}(r_1) \tilde{A}'_{12}^{(JLS)} \times (r_1 r_2; \omega) V_{(JLS)}(r_2) dr_1 dr_2, \quad (20)$$

where \tilde{A}' is calculated with respect to the g.s. $|0'\rangle$ of the final nucleus.

D. Description of $\beta\beta$ decay within the cQRPA

The spectral decomposition of the two-quasiparticle propagator \tilde{A} [Eqs. (9)] can be used for calculation of $\beta\beta$ decay matrix elements in a similar way as described in Sec. II C for $S^{(--)}(\omega)$ [Eq. (19)].

The $2\nu\beta\beta$ decay amplitude $M_{\text{GT}}^{2\nu}$ is defined by the following expression:

$$M_{\text{GT}}^{2\nu} = \sum_s \frac{\langle 0' | \hat{G}^{(-)} | s \rangle \langle s | \hat{G}^{(-)} | 0 \rangle}{\bar{\omega}_s}, \quad (21)$$

where $\hat{G}^{(-)} = \sum_a \sigma_a \tau_a^-$ and again $\bar{\omega}_s = E_s - (E_0 + E_{0'})/2 = (\omega_s^- + \omega_s^+)/2$.

By using the spectral decomposition of Eqs. (9) for $(JLS) = (101)$ and the approximation that the QRPA vacuum $|0'\rangle$ of the final g.s. is the same as $|0\rangle$ of the initial g.s. (the same approximation as used in Refs. [23,24]), the amplitude [Eq. (21)] is simply given by one-half of the corresponding static nuclear polarizability with respect to the external s.p. field $\sigma \tau^-$:

$$M_{\text{GT}}^{2\nu} = -\frac{1}{2} \{\sigma \tilde{A}_{12}(\omega = 0) \sigma\} = -6\pi \int \tilde{A}_{12}^{(101)}(r_1 r_2; \omega = 0) dr_1 dr_2$$

where $\bar{\omega}_s = \omega_s$ is used consistently in this approximation.

The same procedure can be applied to calculate within the cQRPA the matrix element $\langle 0' | \hat{W}^{(--)} | 0 \rangle$ of a two-body scalar operator

$$\hat{W}^{(--)} = \sum_{ab} \mathbf{W}(\mathbf{x}_a, \mathbf{x}_b) \tau_a^{(-)} \tau_b^{(-)}, \quad (22)$$

$$\mathbf{W}(\mathbf{x}_a, \mathbf{x}_b) = \sum_{JLSM} W_{(JLS)}(r_a, r_b) T_{JLSM}(\mathbf{n}_a) T_{JLSM}^*(\mathbf{n}_b),$$

between the ground states $|0\rangle$ and $|0'\rangle$. It is given by a sum of all partial contributions $M^{(JLS)}$:

$$M^{(--)} = -\frac{1}{\pi} \int d\omega \text{Im}\{\mathbf{W}\tilde{A}_{12}(\omega)\} = \sum_{JL} M^{(JLS)}, \quad (23)$$

$$M^{(JLS)} = -\frac{(2J+1)}{\pi} \int d\omega \int W_{(JLS)}(r_1, r_2) \times \text{Im} \tilde{A}_{12}^{(JLS)}(r_1 r_2; \omega) dr_1 dr_2 \quad (24)$$

(where the identification of the ground states as described previously has to be done).

The neutrino potential appearing in the description of the $0\nu\beta\beta$ decay (see, e.g., Refs. [2,3]),

$$\hat{W}_{0\nu}^{(-)} = \sum_{ab} P_v(r_{ab}) \left(\sigma_a \cdot \sigma_b - \frac{g_V^2}{g_A^2} \right) \tau_a^- \tau_b^-, \quad (25)$$

in the simplest Coulomb approximation $P_v(|\vec{r}_a - \vec{r}_b| \equiv r_{ab}) = R/r_{ab}$ (with $R = 1.23 A^{1/3}$ fm being the nuclear radius) has the well-known partial radial components $W_{(JLS)}(r_a, r_b) = \frac{4\pi}{2L+1} \frac{R}{r_{>}} \left(\frac{r_{<}}{r_{>}}\right)^L$ [where $r_{<} = \min(r_a, r_b)$ and $r_{>} = \max(r_a, r_b)$]. When one takes into account both the energy dependence of the neutrino potential $P_v = P_v(r_{ab}, \omega)$ and the usual modification $P_v \rightarrow P_v f_J^2$ with the Jastrow-like function $f_J(r_{ab}) = 1 - e^{-\gamma_1 r_{ab}^2} (1 - \gamma_2 r_{ab}^2)$ to account for the SRC of the two initial neutrons and two final protons, the decomposition of the neutrino potential over the Legendre polynomials P_L can be done numerically:

$$W_{(JLS)}^{0\nu}(r_1, r_2, \omega) = \frac{(2L+1)}{2} \int_0^\pi d \cos \theta_{12} P_L(\cos \theta_{12}) P_v(r_{12}, \omega). \quad (26)$$

In this first application of the cQRPA the corrections from the high-order terms in the nucleonic weak current and the finite nucleon size are omitted, which can lead to a slight overestimation of the calculated $M^{0\nu}$ by 20–30% [7].

Note that, within the cQRPA, in contrast to the discrete QRPA, one does not get an explicit set of QRPA energies and the energy integrations in the expressions for $M^{0\nu}$ [Eqs. (23) and (24)] have to be performed on a mesh. For each point in the energy mesh the cQRPA equations [Eqs. (8)] are solved by discretizing the spatial integrals, thereby transforming them to a matrix representation. All this makes the calculation of $M^{2\nu}$ and $M^{0\nu}$ rather time consuming. Implementation of adaptive integration methods helps to optimize the integration over the energy.

III. CALCULATION RESULTS

We perform the first calculations of the $\beta\beta$ transition amplitudes $M^{2\nu}$ and $M^{0\nu}$ within the cQRPA for ^{76}Ge , ^{100}Mo , and ^{130}Te . We also compare the results obtained with those calculated within the usual “discrete” version of the QRPA to see the influence of the single-particle continuum.

For the first calculations of $M^{2\nu}$ and $M^{0\nu}$ within the continuum QRPA we adopt a rather simple nuclear Hamiltonian similar to that used in Refs. [23,24]. The chosen nuclear mean field $U(x)$ consists of the phenomenological isoscalar part $U_0(x)$ along with the isovector $U_1(x)$ and the Coulomb $U_C(x)$ parts, both calculated consistently in the Hartree approximation (see Ref. [13]). The residual isovector particle-hole interaction and the particle-particle interaction in both the neutral (pairing) and charge-exchange channels are

chosen in the form of zero-range forces [Eqs. (10)–(12)]. All the strength parameters of the residual interactions are given in units of 300 MeV fm³.

The results calculated within the discrete QRPA, labeled A, B, and C, refer to the different s.p. bases used. Case A corresponds to the large s.p. basis in the calculations: 16 successive s.p. levels comprising $N = 1-5$ major Saxon-Woods shells for ^{76}Ge and ^{100}Mo and 22 successive s.p. levels (all bound s.p. states for neutrons and all bound s.p. states along with 6 quasistationary states for protons) comprising $N = 1-6$ major shells for ^{130}Te . Note that the same s.p. basis is used within the cQRPA as in the BCS problem. Case B corresponds to the small s.p. basis and is obtained from A by subtracting the six lowest s.p. levels comprising $N = 1-3$ major shells (inert core of ^{40}Ca). Case C corresponds to the solution of the QRPA equations in the large basis A, in which, however, the BCS problem is solved in the small basis B (i.e., the Bogolyubov coefficients $v_\alpha = 1$ are taken for the six lowest s.p. levels). This tests the approximations involved in the current cQRPA calculations, namely, that v_α is set exactly to zero for the s.p. states lying above the BCS basis.

Fixing the model parameters is done in the following way:

- (i) The p-h isovector strength f_{ph}^0 is chosen equal to unity ($f_{\text{ph}}^0 = 1.0$). This allows reproduction of the experimental nucleon binding energies for closed-shell nuclei by implementing the isospin self-consistency of the symmetry potential $U_1(x)$ of the mean field with the isovector p-h interaction (see Ref. [13]).
- (ii) The p-h spin-isovector strength f_{ph}^1 is fitted to reproduce the experimental energy of the GTR.
- (iii) The pairing strengths g_n^{pair} and g_p^{pair} are fixed within the BCS model to reproduce the experimental pairing energies. As already mentioned, all the other strength parameters in the particle-particle channel are given relative to $(g_n^{\text{pair}} + g_p^{\text{pair}})/2$.
- (iv) By choosing the p-p isovector strength $g_{\text{pp}}^0 = 1.0$ we restore approximately the isospin self-consistency of the total residual p-p interaction.
- (v) The p-p spin-isovector strength g_{pp}^1 is chosen to reproduce the experimental (positive) value of $M^{2\nu}$ as done in Refs. [6,7].

In Fig. 1 the calculated g_{pp}^1 dependence of $M^{2\nu}$ is plotted. Calculated $M^{2\nu}$ depends on the choice of the g.s. (either initial or final) with respect to which the QRPA equations are solved. It can be seen in the figure that the $M^{2\nu}$ calculated within the discrete QRPA and the cQRPA are almost the same at small values of g_{pp}^1 , though the difference becomes visible while g_{pp}^1 grows. Thus, the correction to the $M^{2\nu}$ coming from the s.p. continuum is small, as can be expected for the Gamow-Teller transitions.

The values of the strength parameters f_{ph}^1 and g_{pp}^1 fixed according to our prescription are listed in Table I for both the discrete and continuum versions of the QRPA. Because calculated $M^{2\nu}$ depends on the choice of the g.s. (either initial or final) with respect to which the QRPA equations are solved, two sets of g_{pp}^1 are obtained. The upper and lower lines for each decay sequence in Table I contain g_{pp}^1 fitted for initial

TABLE I. Choice of the model parameters. See text for explanation of the choices A, B, and C for different model spaces within the discrete QRPA. The two lines for the parameters of g_{pp}^1 for each $\beta\beta$ decay are fitted by using the QRPA set of the intermediate states built with respect to the g.s. of the initial nucleus (e.g., ^{76}Ge) and the g.s. of the final nucleus (e.g., ^{76}Se). The p-h strength f_{pp}^1 is adjusted to reproduce the energy of the Gamow-Teller resonance in the initial nucleus (e.g., ^{76}Ge).

Nuclear transition	$M_{\text{exp}}^{2\nu}$ (MeV $^{-1}$)	Strength parameters	Discrete QRPA			Continuum QRPA
			A	B	C	
$^{76}\text{Ge} \rightarrow ^{76}\text{Se}$	0.15	g_{pp}^1	0.98	0.97	0.97	0.91
		g_{pp}^1	1.10	1.10	1.10	1.01
		f_{ph}^1	0.40	0.43	0.43	0.40
$^{100}\text{Mo} \rightarrow ^{100}\text{Ru}$	0.24	g_{pp}^1	1.28	1.31	1.30	1.10
		g_{pp}^1	1.43	1.50	1.49	1.23
		f_{ph}^1	0.70	0.70	0.70	0.75
$^{130}\text{Te} \rightarrow ^{130}\text{Xe}$	0.03	g_{pp}^1	1.23	1.25	1.25	1.11
		g_{pp}^1	1.25	1.28	1.28	1.13
		f_{ph}^1	0.60	0.60	0.60	0.63

and final nuclei, respectively. One sees that the difference in the obtained g_{pp}^1 is almost negligible for $^{130}\text{Te} \rightarrow ^{130}\text{Xe}$, but it becomes $\delta g_{pp}^1 \approx 0.2$ for $^{100}\text{Mo} \rightarrow ^{100}\text{Ru}$.

The calculated values of $M^{0\nu}$ are given in Table II for both versions of the QRPA for $g_A = 1.25$. The numbers in parentheses are the matrix elements calculated with inclusion of the SRC in terms of the Jastrow-like function. The two lines of results for each $\beta\beta$ decay chain contain $M^{0\nu}$ calculated with respect to the g.s. of the initial or final nucleus in the decay (see Sec. IID). In the present first application of the cQRPA, neither the finite nucleon size nor the higher order

terms of the nucleon current are considered. (They usually bring a additional reduction of $M^{0\nu}$ by about 30%; see, e.g., Ref. [7].)

The contribution of multipoles with $L = 0-5$ are included in the calculations of $M^{0\nu}$. The contributions with $L > 5$ (which can increase $M^{0\nu}$ in total by about 10%) are omitted here as the corresponding parts in the transition operator probe the short-range behavior of the nucleon-nucleon wave function that cannot be well described within the QRPA. It is known that the RPA in medium is formulated to describe propagation of small-amplitude density fluctuations and only the ring diagrams are summed (see, e.g., Ref. [25]). This is a quite suitable approximation to deal with collective long-wave excitations, but for the short-range ones the diagrams that are left out of the RPA method become important.

As one sees from comparison of the discrete QRPA results listed in columns A and B, the calculated $M^{0\nu}$ values for different basis sizes come out very close to each other provided

TABLE II. $0\nu\beta\beta$ nuclear matrix elements evaluated without and with (in parentheses) the SRC in both discrete and continuum QRPA. See text for explanation of the choices A, B, and C for different model spaces within the discrete QRPA. The two lines of results for each $\beta\beta$ decay contain $M^{0\nu}$ calculated by using the QRPA set of the intermediate states built with respect to the g.s. of the initial nucleus (e.g., ^{76}Ge) and the g.s. of the final nucleus (e.g., ^{76}Se).

Nuclear transition	Discrete QRPA			Continuum QRPA
	A	B	C	
$^{76}\text{Ge} \rightarrow ^{76}\text{Se}$	5.95 (4.30)	5.63 (4.19)	4.30 (3.19)	4.30 (3.09)
	5.44 (3.86)	5.22 (3.82)	3.81 (2.76)	3.63 (2.46)
$^{100}\text{Mo} \rightarrow ^{100}\text{Ru}$	5.52 (3.88)	5.35 (3.84)	4.24 (3.00)	2.49 (1.67)
	4.19 (2.73)	4.00 (2.65)	2.91 (1.84)	1.39 (0.67)
$^{130}\text{Te} \rightarrow ^{130}\text{Xe}$	3.17 (2.19)	3.14 (2.20)	2.56 (1.78)	1.70 (1.12)
	4.69 (3.21)	4.67 (3.21)	3.77 (2.57)	2.03 (1.28)

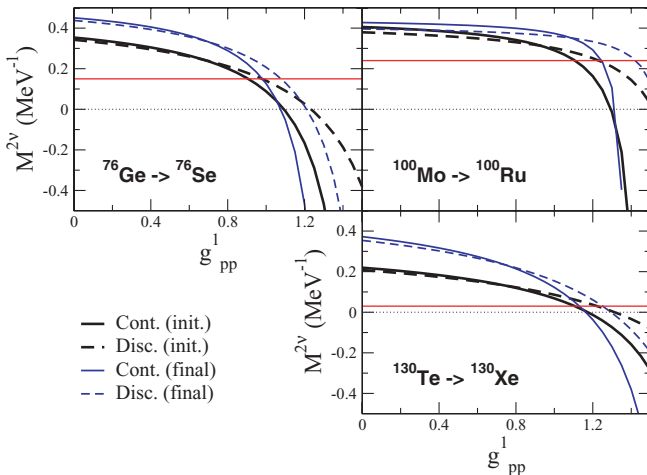


FIG. 1. (Color online) The calculated dependence of the $2\nu\beta\beta$ matrix element on the p-p strength g_{pp}^1 in both discrete (set A, dashed lines) and continuum QRPA (solid lines). The calculations performed by using the QRPA set of the intermediate states built with respect to the g.s. of the initial nucleus (e.g., ^{76}Ge) and the g.s. of the final nucleus (e.g., ^{76}Se) are depicted by thick and thin lines, respectively. The solid horizontal line gives the (positive) experimental value of the $2\nu\beta\beta$ decay matrix elements used in the calculation to fit g_{pp}^1 .

the p-p interaction parameter g_{pp}^1 is fixed to reproduce the experimental $2\nu\beta\beta$ decay matrix elements $M_{\text{exp}}^{2\nu}$. This result provides an independent confirmation of the main conclusion of Ref. [7], which is obtained here for a different nuclear Hamiltonian and by solving the pn-QRPA equations in the coordinate representation. Also, the $M^{0\nu}$ values obtained by using only the initial QRPA g.s. (upper line) or final one (lower line) in the calculation are rather closer to each other.

The matrix elements $M^{0\nu}$ calculated by taking into account the SRC in terms of the Jastrow functions get suppressed by about 25–30% in the present calculation, which is in quantitative agreement with other recent calculations [7,16] but do not support the old results of Ref. [24] where the strong suppression was found. However, one should keep in mind that this way of describing the SRC can be rather rough and can lead to overestimation of the suppression of the $M^{0\nu}$. Other methods for describing the SRC such as UCOM [26] give much less suppression in the calculated $M^{0\nu}$ (only about 10%) and this important issue is currently under intensive study [14,16].

The matrix elements $M^{0\nu}$ calculated within the cQRPA (the last column of Table II) are systematically smaller than the discrete QRPA ones (columns A and B). The suppression varies from about 30% for ^{76}Ge to a factor 2 for ^{100}Mo and ^{130}Te . The origin of this suppression can be associated with additional g.s. correlations appearing because of highly excited collective states embedded in the s.p. continuum. Transitions to these states are naturally described within the cQRPA in terms of the s.p. Green's functions (see Sec. II B). However, the applied version of the cQRPA in this work does not include nucleon pairing in the s.p. continuum, and therefore the $M^{0\nu}$ values obtained here should be treated only as lower limits. Inclusion of nucleon pairing in the s.p. continuum (which is a formidable task) will definitely lead to an increase of the matrix elements within the cQRPA. To demonstrate the importance of nucleon pairing far from the Fermi level for quantitative description of the $M^{0\nu}$, the numbers listed in column C of Table II can be compared with those in columns A and B. Case C is introduced, as previously described, to test within the discrete QRPA the neglect of pairing far from the Fermi level, in a manner similar to how it is done in the present version of the cQRPA. Inspecting column C, one sees a marked reduction, by about 30%, in the calculated $0\nu\beta\beta$ matrix elements. Thus, expanding the discrete QRPA basis from the “small” one of B to a large one of C, which neglects pairing effects in the inert core but allows transitions from the inert core, leads to a suppression in the $M^{0\nu}$ because of more g.s. correlations. The suppression, however, gets almost completely compensated as nucleon pairing is switched on in the inert core and one goes from case C to case A. The same sort of compensation is natural to expect in the case of the cQRPA when nucleon pairing is

switched on in the single-particle continuum. However, one cannot exclude that the compensation is incomplete.

Let us conclude with some words about possible prospects for taking nucleon pairing in the s.p. continuum into consideration within the approach described in here. Though possible ways of treating the continuum pairing within the QRPA can be found in the literature (see, e.g., Ref. [17]), direct implementation of them would drastically increase the corresponding calculation efforts. One would need first to calculate the solutions $u(r)$ and $v(r)$ of the coordinate Hartree-Fock-Bogolyubov equation for positive energies, from which then additional continuum contributions to the expressions [Eqs. (13)] for the response function should be constructed by direct integration over energy. Probably, a more economical way is to discretize the continuum by putting the nucleus in a large box. These further developments are postponed to a future publication that should then finally answer the question about stability of $M^{0\nu}$ with respect to the basis size.

IV. CONCLUSIONS

A continuum QRPA approach to calculation of the nuclear double beta decay $2\nu\beta\beta$ and $0\nu\beta\beta$ amplitudes has been formulated. Calculations of the amplitudes $M^{2\nu}$ and $M^{0\nu}$ within the cQRPA are performed for ^{76}Ge , ^{100}Mo , and ^{130}Te . A rather simple nuclear Hamiltonian consisting of phenomenological mean field and zero-range residual particle-hole and particle-particle interaction is used. The $M^{2\nu}$ values are almost unaffected when the single-particle continuum is taken into account. In contrast, we find a regular suppression of the $0\nu\beta\beta$ amplitude that can be associated with additional ground-state correlations owing to collective states in the continuum. The calculated $M^{0\nu}$ values of this paper should be considered as lower limits for the matrix elements within the cQRPA, as nucleon pairing is realized only on a discrete basis within the present version of the cQRPA. It is expected that future inclusion of nucleon pairing in the single-particle continuum will somewhat compensate the observed suppression of $M^{0\nu}$ values.

ACKNOWLEDGMENTS

We are grateful to Mrs. L. Rodina for helping us with implementation of an adaptive integration procedure in the numerical solution of the continuum QRPA equations. We also thank Prof. M. Urin for valuable discussions. The work is supported in part by the Deutsche Forschungsgemeinschaft (Grant No. FA67/28-2 within the Transregio Project TR27 “Neutrinos and Beyond”) and by the EU ILIAS project (Contract No. RII3-CT-2004-506222).

-
- [1] R. D. McKeown and P. Vogel, Phys. Rep. **394**, 315 (2004).
 [2] A. Faessler and F. Šimkovic, J. Phys. G **24**, 2139 (1998).
 [3] J. Suhonen and O. Civitarese, Phys. Rep. **300**, 123 (1998).
 [4] S. R. Elliott and P. Vogel, Annu. Rev. Nucl. Part. Sci. **52**, 115 (2002).
 [5] S. R. Elliott and J. Engel, J. Phys. G **30**, R183 (2004).

- [6] V. A. Rodin, A. Faessler, F. Šimkovic, and P. Vogel, Phys. Rev. C **68**, 044302 (2003).
 [7] V. A. Rodin, A. Faessler, F. Šimkovic, and P. Vogel, Nucl. Phys. A **766**, 107 (2006); erratum-*ibid.* A **793**, 213 (2007).
 [8] S. Schlomo and G. Bertsch, Nucl. Phys. A **243**, 507 (1975).

- [9] S. E. Muraviev and M. H. Urin, Nucl. Phys. **A572**, 267 (1994); E. A. Moukhai, V. A. Rodin, and M. H. Urin, Phys. Lett. **B447**, 8 (1999); V. A. Rodin and M. H. Urin, *ibid.* **B480**, 45 (2000); M. L. Gorelik, S. Shlomo, and M. H. Urin, Phys. Rev. C **62**, 044301 (2000); V. A. Rodin and M. H. Urin, Nucl. Phys. **A687**, 276c (2001).
- [10] N. Auerbach and A. Klein, Nucl. Phys. **A422**, 480 (1984); O. N. Vyazankin and M. H. Urin, *ibid.* **A537**, 534 (1992); E. Kolbe, K. Langanke, and P. Vogel, Phys. Rev. C **62**, 055502 (2000).
- [11] E. Kolbe, K. Langanke, G. Martinez-Pinedo, and P. Vogel, J. Phys. G **29**, 2569 (2003).
- [12] I. N. Borzov, E. L. Trykov, and S. A. Fayans, Sov. J. Nucl. Phys. **52**, 627 (1990); I. N. Borzov, S. A. Fayans, and E. L. Trykov, Nucl. Phys. **A584**, 335 (1995).
- [13] V. A. Rodin and M. H. Urin, Phys. At. Nucl. **66**, 2128 (2003).
- [14] F. Šimkovic, A. Faessler, V. A. Rodin, P. Vogel, and J. Engel, arXiv:0710.2055 [nucl-th].
- [15] G. A. Miller and J. E. Spencer, Ann. Phys. (NY) **100**, 562 (1976).
- [16] M. Kortelainen, O. Civitarese, J. Suhonen, and J. Toivanen, Phys. Lett. **B647**, 128 (2007); M. Kortelainen and J. Suhonen, Phys. Rev. C **75**, 051303(R) (2007); **76**, 024315 (2007).
- [17] M. Matsuo, Nucl. Phys. **A696**, 371 (2001); E. Khan, N. Sandulescu, M. Grasso, and N. Van Giai, Phys. Rev. C **66**, 024309 (2002).
- [18] I. N. Borzov and S. Goriely, Phys. Rev. C **62**, 035501 (2000); I. N. Borzov, Nucl. Phys. **A777**, 645 (2006).
- [19] V. A. Rodin, M. H. Urin, and A. Faessler, Nucl. Phys. **A747**, 297 (2005).
- [20] V. Rodin and A. Faessler, Prog. Part. Nucl. Phys. **57**, 226 (2006).
- [21] P. Ring and P. Schuck, *The Nuclear Many-Body Problem* (Springer-Verlag, Berlin, 1980).
- [22] A. B. Migdal, *Theory of Finite Fermi-Systems and Properties of Atomic Nuclei* (Nauka, Moscow, 1983) [in Russian].
- [23] P. Vogel and M. R. Zirnbauer, Phys. Rev. Lett. **57**, 3148 (1986).
- [24] J. Engel, P. Vogel, and M. R. Zirnbauer, Phys. Rev. C **37**, 731 (1988).
- [25] A. L. Fetter and J. D. Walecka, *Quantum Theory of Many-Particle Systems* (McGraw-Hill, New York, 1971).
- [26] R. Roth, H. Hergert, P. Papakonstantinou, T. Neff, and H. Feldmeier, Phys. Rev. C **72**, 034002 (2005); R. Roth, P. Papakonstantinou, N. Paar, H. Hergert, T. Neff, and H. Feldmeier, *ibid.* **73**, 044312 (2006).